A surface plasmon resonance sensor based on a multi-core photonic crystal fiber*

ZHANG Pei-pei (张培培)[1,2]**, **YAO Jian-quan** (姚建铨)[1,2], **CUI Hai-xia** (崔海霞)[1,2], **and LU Ying** (陆颖)[1,2]

1. *Institute of Laser & Optoelectronics, College of Precision Instruments and Opto-Electronic Engineering, Tianjin University, Tianjin 300072, China*
2. *Key Laboratory of Opto-electronics Information and Technical Science, Ministry of Education, Tianjin University, Tianjin 300072, China*

(Received 18 March 2013)

A surface plasmon resonance (SPR) sensor based on a multi-core photonic crystal fiber (PCF) is presented in this paper. There is only one analyte channel positioned in the center of the PCF cross section, rather than several closely arranged analyte channels around the central core. So the design of this sensor not only reduces the consumption of gold and samples, but also effectively avoids the interference between neighboring analyte channels. Optical field distributions of this fiber at different wavelengths and the sensing properties of this sensor are theoretically analyzed and discussed using finite element method (FEM). Simulation results confirm that both the thickness of metallic layer and the fiber structural parameters have significant effect on sensing performance. The amplitude sensitivity of the sensor is found to be 1.74×10^{-5} RIU, and the spectral sensitivity is 3300 nm/RIU, corresponding to a resolution of 3.03×10^{-5} RIU. Finally, in order to achieve PCF-SPR sensing characteristics, an experiment design scheme based on spectroscopic detection method is proposed.

Document code: A **Article ID:** 1673-1905(2013)05-0342-4
DOI 10.1007/s11801-013-3052-0

Surface plasmon resonance (SPR) exists between the metal and dielectric (or air). The SPR sensing technology has become the research focus in the biochemical sensing field[1-5], because of its high sensitivity, without background interference, labelfree sample, without further purification, real-time rapid detection, etc.

Photonic crystal fibers (PCFs) or hollow fibers (HFs) with a regular hexagonal array of holes along the propagation direction have promoted the development of fiber optic SPR sensors. Compared with other types of SPR sensors, PCF-based SPR sensing technology has a number of advantages, such as multi-dimensional structure, large mode area, multi-parameter measurement and wide tuning range[6-12]. In recent years, many types of PCF-SPR sensors have been designed for liquid and gas detection. Hassani and Skorobogatiy[13,14] analyzed the design principles for two different PCF structures with metallic coating for biosensing applications in detail. Recently, Mikhail Erdmanis et al[15] proposed an H-shaped optical fiber. In their design, the two U-shaped grooves are firstly coated with a thin gold layer and then covered by a uniform titanium dioxide layer to facilitate spectral tuning of the device. And they finally obtained a refractive-index resolution up to 5×10^3 nm/RIU. Chi Zhou et al[16] presented a special sensor design with hybrid mechanisms based on a PCF in which there are two analyte channels.

In this paper, a design of optical SPR sensor utilizing the index-guiding multi-core PCF is proposed, and a comprehensive numerical characterization based on the finite element method (FEM) is presented. Different from previous structures, there is only one analyte channel positioned in the center of the multi-core PCF cross section, rather than several closely arranged analyte channels around the central core. The novel design has the following advantages. Firstly, it is less time-consuming to coat and infiltrate the analyte channel, and the consumption of gold and analyte is greatly reduced at the same time. Secondly, the six identical solid cores can feature a C_{6v} rotational symmetry with respect to the metalized analyte channel, which guarantees a polarization independent propagation characteristic. Thirdly, the interference between neighboring analyte channels can be effectively eliminated. Finally, Binbin Shuai et al[17] confirmed that this multi-core PCF sensor has a broad analyte refractive index range from 1.33 to 1.53. The large dynamic detection range makes it more competitive in the biological, chemical and industrial applications.

The structure of the multi-core PCF based SPR sensor is shown in Fig.1(a) and the fundamental mode field dis-

* This work has been supported by the Major State Basic Research Development Program of China (No.2010CB327801).
** E-mail: chinahebei2010@126.com

tribution is shown in Fig.1(b). It consists of three air hole layers arranged in a hexagonal way, and the cores are formed by omitting corresponding air holes in the second layer, which are substituted by six silica rods. The pitch of the underlying hexagonal lattice is Λ=2 μm, and the diameters of the central analyte channel and cladding air holes are d_c=0.8Λ and d=0.5Λ, respectively. The thickness of gold layer is t_{Au} = 40 nm. The PCF is made of silica glass with the refractive index of 1.45, cladding holes are filled with air (n=1.0), while metalized microchannel is infiltrated with aqueous sample with n_a=1.42. The dielectric constant of gold in the visible and near infrared (NIR) region is defined by the Drude model[18].

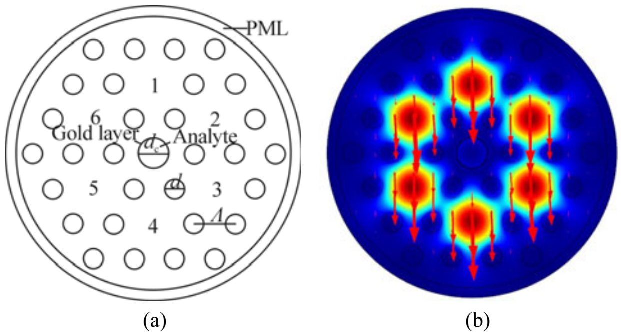

Fig.1 (a) Schematic diagram of the multi-core PCF based SPR sensor; (b) Optical field distribution of the fundamental mode, where the arrow indicates the polarization direction of magnetic field

The finite element method (FEM) with a perfectly matched layer (PML) is chosen to calculate the effective indices of electromagnetic mode in complex domain. When the plasmon resonance occurs, the imaginary part of the mode refractive index will change dramatically. Fig.2 shows the distribution of the refractive index of the sensor, and it indicates that the imaginary part of the refractive index shows a significant shock peak when the incident wavelength is 750 nm. The real part of the mode effective refractive index in plural form is the concept of the refractive index in the usual sense, and the imaginary part describes the mode loss. The energy loss of core guided mode is mainly due to its excitation generating the surface plasmon mode. Fig.2 illustrates that the core guided mode and the plasma mode produce a resonance at the wavelength of 750 nm, as shown in the inset of Fig.2. Multi-mode fiber optic SPR sensor often presents a plurality of formats because of the different propagation constants, the modes transferred in the core of the fiber are likely to meet the phase matching condition and produce the class surface plasma oscillations, and the resonance wavelengths of different modes are different. Considering most of the energy of the optical fiber transferred in the form of fundamental mode, here we mainly consider the surface plasmon resonance stimulated by the fundamental mode.

The confinement loss is proportional to the imaginary part of its effective index, and can be expressed as $\alpha = 40\pi\,\mathrm{Im}(n_{eff})/(\ln 10)\lambda$, where λ is the wavelength in meters, and Im(n_{eff}) is imaginary part of refractive index in the fundamental mode. The excitation of surface plasmon can be characterized by calculating the loss of the optical fiber.

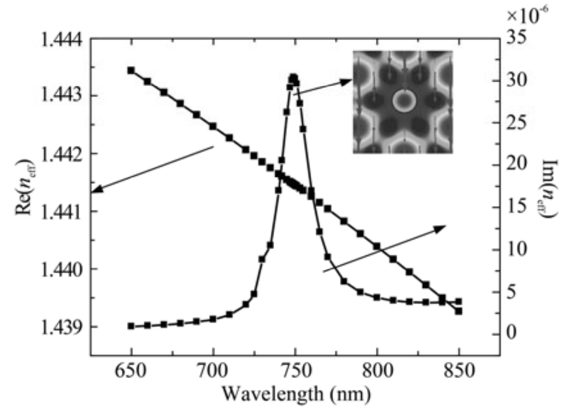

Fig.2 Distribution of the refractive index of the sensor

Being surface excitations, surface plasmon waves are very sensitive to the thickness of metallic layer. Therefore, the changes in the spectra for the plasmonic peak are investigated when the thickness of gold t_{Au} is varied from 30 nm to 50 nm. As can be seen in Fig.3, the confinement loss at resonance wavelength decreases, while the thickness of metal layer increases, and the center wavelength of the peak moves toward the longer wavelengths. This feature can be used to detect the changes of the thickness of thin biolayer deposited on the top of the metal film in biosensor[13].

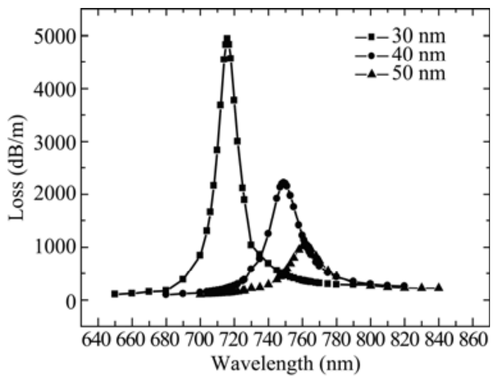

Fig.3 Loss spectra of the SPR sensor with the thickness of metal layer varying from 30 nm to 50 nm

Furthermore, the influence of the fiber geometry on the sensing performance is shown in Fig.4. d_c is varied from 0.75Λ to 0.85Λ while keeping all other structural parameters constant. An increase in the confinement loss of the core guided mode can be observed for the larger size of the central hole. It can be explained by that larger size hole in the center makes metallic surface closer to the mode field. It leads to the increased contact area between mode field and metallic surface and more light coupled to metallic surface in turn, hence introduces higher propagation losses. The increase of d_c also leads to a red shift of the resonance wavelength.

Fig.4(b) shows the *d*-dependent loss properties. It can be seen that there is an overall increase in the plasmonic resonant loss of the core guided mode as *d* decreases. It is easy to understand by that the decrease of the size of holes in the outer layer promotes the leakage of the modal field from the fiber core, resulting in worse confinement to the core. This ultimately leads to the enhanced coupling between the core guided mode and plasmonic mode. In addition, it demonstrates that the resonance wavelength is not affected by the outer holes size.

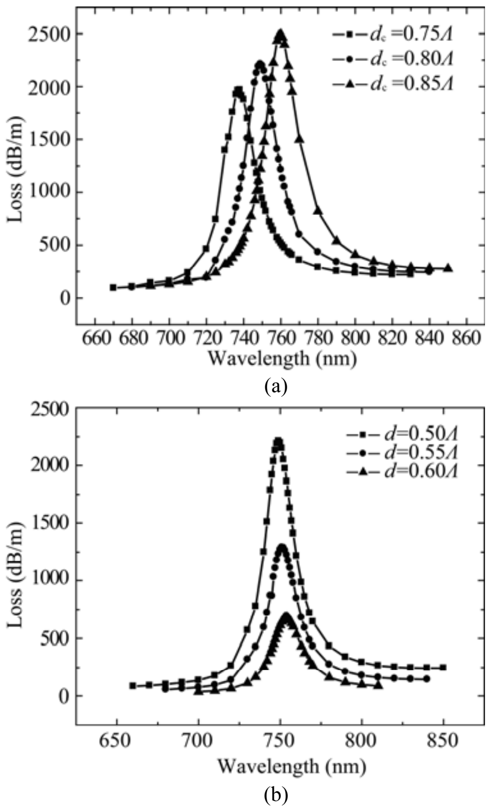

Fig.4 The influence of the diameters of (a) central hole and (b) outer holes in the fiber on the loss of a core guided mode assuming d_c=0.8Λ, *t*=40 nm, n_a=1.42

From Fig.4, it can be seen that the size of central hole (d_c) has a significant effect on the resonance wavelength, but the size of outer holes (*d*) has a great effect on the resonance peak intensity. Through adjusting the size of the central hole, the resonance wavelength can be tuned to a desired value. And its length is limited to several centimeters due to the high loss of PCF based SPR sensor. Therefore, such a sensor should be considered as an integrated photonic element.

For a sensor, sensitivity is one of the most important parameters, which means the variation in the ratio of the SPR resonance parameters (wavelength, amplitude, etc.) and the refractive index of the samples. Here two methods are used to detect the changes of the refractive index in the sample. One is known as amplitude detection at a single wavelength. Assume that the wavelength of incident light is λ, and the propagation length is L, then the amplitude detection sensitivity for refractive index variation Δn_a can be defined as:

$$S_{\mathrm{A}}\left(\mathrm{RIU}^{-1}\right)=[P\left(L,\lambda,n_{\mathrm{a}}+\Delta n_{\mathrm{a}}\right)-P\left(L,\lambda,n_{\mathrm{a}}\right)]/P\left(L,\lambda,n_{\mathrm{a}}\right)/\Delta n_{\mathrm{a}}\ . \quad (1)$$

If $L=1/\alpha(\lambda,n_{\mathrm{a}})$, the amplitude detection sensitivity of the analyte refractive index can be defined as[14]:

$$S_{\mathrm{A}}\left(\lambda\right)=[\partial\alpha\left(\lambda,n_{\mathrm{a}}\right)/\partial n_{\mathrm{a}}]/\alpha\left(\lambda,n_{\mathrm{a}}\right). \quad (2)$$

Another is the method of wavelength scanning. By detecting the shift of the peak position ($\Delta\lambda_{\mathrm{p}}$) for the change of the analyte refractive index (Δn_{a}), the spectral sensitivity can be calculated by[14]:

$$S_{\lambda}(\mathrm{nmRIU}^{-1})=\Delta\lambda_{\mathrm{p}}/\Delta n_{\mathrm{a}}\ . \quad (3)$$

Fig.5(a) depicts the corresponding shift in the resonant attenuation peak by changing the analyte refractive index from 1.41 to 1.42. And there is a sharp loss peak in the range from 710 nm to 760 nm, due to the resonance between the core mode and the surface plasmon makes great energy loss of light field in the core. The resonance peak shifts to the longer wavelengths as the analyte index increases, and the refractive index change (Δn_{a}) of 0.01 results in a 33 nm shift of the loss peak ($\Delta\lambda_{\mathrm{p}}$), which means the sensitivity of the sensor is 3300 nm/RIU. If the peak wavelength resolution of the instrument is assumed to be $\Delta\lambda_{\min}$=0.1 nm, the refractive index resolution of corresponding sensor can be 3.03×10^{-5} RIU. Fig.5(b) presents the amplitude sensitivity of the fiber based SPR sensor. It can be seen that the maximal sensitivity is 575

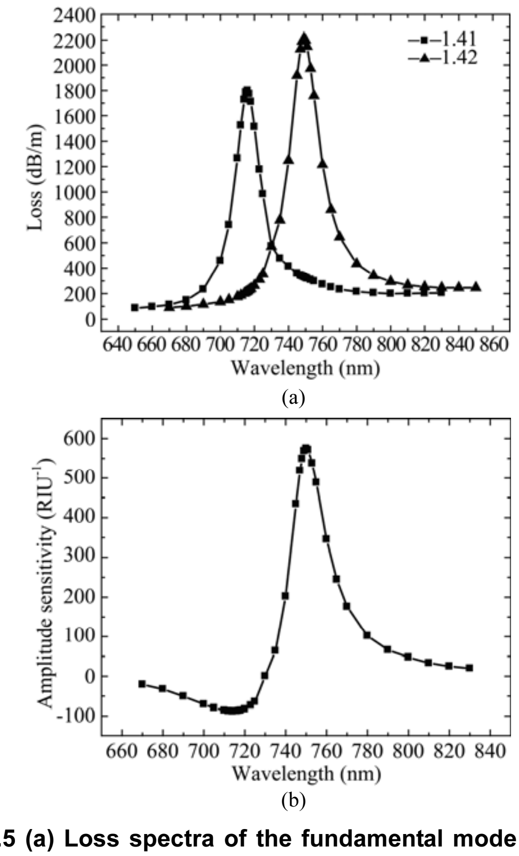

Fig.5 (a) Loss spectra of the fundamental mode with two different refractive indices of the sample; (b) Amplitude sensitivity of the sensor

RIU^{-1} which is achieved at 750 nm. Assuming that the change in the transmitted intensity of 1% can be detected reliably, the sensor resolution of 1.74×10^{-5} RIU can be predicted.

By the above simulation analyses, it is found that sensitivity of magnitude detection method has large variation with wavelength alteration, and the measurement of SPR sensing characteristics of PCF based on different structures requires the laser with different output wavelengths, and it has more stringent requirements on the laser output power and the efficiency of coupling device. In comparison, the spectrum detection method can take advantage of a broadband light source as spectral scanning probe and easy to achieve all-fiber structure measurement.

Sensing experimental setup is shown in Fig.6. The specific measurement procedure is as follows. Firstly, the beam with wide spectrum output by the broadband light source is through an isolator to choose light, and then is coupled into the ordinary single mode optical fiber through optical connector. Then, the input beam is divided into two beams uniformly through a 3 dB coupler. A beam of light as a reference is input into the spectrometer through the uncoated PCF, and the other beam of light as sample is input into the spectrometer through the coated PCF. Finally, a computer is used to analyze spectral data collected by the spectrometer, and the sample parameters are obtained. In the measurement process, the reference fiber and experimental fiber are filled with the same tested solution, and the resonant absorption peak (resonance wavelength) can be observed by detecting and comparing the spectra of the two signals. Filling samples with different refractive indices will cause the resonance wavelength to move, therefore, the information of the test sample can be obtained according to the changes of the resonance wavelength.

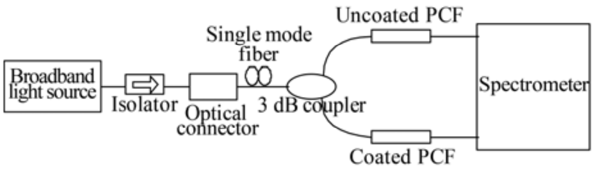

Fig.6 PCF-SPR sensing experimental setup

A multi-core PCF-SPR sensor with six identical solid cores around one metalized analyte channel is shown in this paper. The novel design is with only one analyte channel positioned in the center of the PCF cross section, rather than several closely arranged analyte channels around the central core, which not only reduces the consumption of gold and sample, but also effectively avoids the interference between neighboring analyte channels. The loss spectra and sensitivity of the proposed sensor are calculated using the FEM with PML. Simulation results reveal that both the thickness of metallic layer and the fiber structural parameters have significant effect on sensor performance. Assuming that 1% amplitude change can be detected, the detection limit of the amplitude-based sensor for measuring index changes of the liquid analyte at 750 nm is found to be 1.74×10^{-5} RIU. The detection sensitivity of the same sensor in the wavelength scanning is predicted to be 3300 nm/RIU, which is 3.03×10^{-5} RIU with detection limit of 0.1 nm in the shift of a plasmonic peak. Thus sensing sensitivities of the sensor proposed in this paper are comparable to those of existing fiber sensor structures. Finally, a PCF-SPR sensing experiment design based on spectroscopic detection method is proposed. The design with all-fiber optical system possesses high stability and good reliability, and is applicable to measure many samples.

References

[1] Liedberg B., Nylander C. and Lunstrom I., Sensors and Actuators **4**, 299 (1983).
[2] C. Nylander, B. Liedberg and T. Lind, Sensors and Actuators **3**, 79 (1982).
[3] Kabashin A.V. and Nikitin P. I., Opt. Commun. **150**, 5 (1998).
[4] Sookyoung R., Taerin C. and Byoungho L., Sensors **11**, 1565 (2011).
[5] Yong C. and Hai M., Photonic Sensors **2**, 37 (2012).
[6] J. W. Xing, S. Zhu, T. Y. Wang, N. Chen and Z. Y. Chen, J. Optoelectron. Laser **22**, 693 (2011). (in Chinese)
[7] Hautakorpi M., Mattinen M. and Ludvigsen H., Opt. Express **16**, 8427 (2008).
[8] BING Pi-bin, LI Zhong-yang, YAO Jian-quan, LU Ying, DI Zhi-gang and YAN Xin, Optoelectronics Letters **8**, 245 (2012).
[9] Yating Zhang, Li Xia, Chi Zhou, Xia Yu, Hairong Liu, Deming Liu and Ying Zhang, Opt. Commun. **284**, 4161 (2011).
[10] Ying Lu, Cong-Jing Hao, Bao-Qun Wu, Xiao-Hui Huang, Wu-Qi Wen, Xiang-Yong Fu and Jian-Quan Yao, Sensors **12**, 12016 (2012).
[11] Xia Yu, Ying Zhang, Shanshan Pan, Ping Shum, Min Yan, Yehuda Leviatan and Changming Li, J. Opt. **12**, 1 (2010).
[12] Wei Wei, Xia Zhang, Xin Guo, Long Zheng, Jing Gao, Weipeng Shi, Qi Wang, Yongqing Huang and Xiaomin Ren, Optik **123**, 1167 (2012).
[13] Hassani A. and Skorobogatiy M., Opt. Express **14**, 11616 (2006).
[14] Hassani A. and Skorobogatiy M., J. Opt. Soc. Am. B **24**, 1423 (2007).
[15] Mikhail Erdmanis, Diana Viegas, Markus Hautakorpi, Steffen Novotny, José Luis Santos and Hanne Ludvigsen, Opt. Express **19**, 13980 (2011).
[16] Chi Zhou, Yating Zhang, Li Xia and Deming Liu, Opt. Commun. **285**, 2466 (2012).
[17] Binbin Shuai, Li Xia, Yating Zhang and Deming Liu, Opt. Express **20**, 5974 (2012).
[18] Elkin N. N., Napartovich A. P., Troshchieva V. N. and Vysotsky D. V., J. Lightwave Technol. **25**, 3072 (2007).